

Roles of Semaphorin-6B and Plexin-A2 in Lamina-Restricted Projection of Hippocampal Mossy Fibers

Hiroshi Tawarayama,^{1,2} Yutaka Yoshida,^{3,4} Fumikazu Suto,^{5,6,7} Kevin J. Mitchell,² and Hajime Fujisawa¹

¹Division of Biological Science, Nagoya University Graduate School of Science, Chikusa-ku, Nagoya 464-8602, Japan, ²Smurfit Institute of Genetics, and Institute of Neuroscience, Trinity College Dublin, Dublin 2, Ireland, ³Howard Hughes Medical Institute, Department of Biochemistry and Molecular Biophysics, Center for Neurobiology and Behavior, Columbia University, New York, New York 10032, ⁴Division of Developmental Biology, Cincinnati Children's Hospital Medical Center, Cincinnati, Ohio 45229, ⁵Division of Developmental Neuroscience, Center for Translational and Advanced Animal Research, Tohoku University Graduate School of Medicine, Sendai, 980-8575, Japan, ⁶Division of Developmental Genetics, National Institute of Genetics, Mishima 411-8540, Japan, and ⁷Core Research for Evolutional Science and Technology, Japan Science and Technology Agency, Kawaguchi 332-0012, Japan

Hippocampal mossy fibers project preferentially to the proximal-most lamina of the suprapyramidal region of CA3, the stratum lucidum, and proximal-most parts of the infrapyramidal region of CA3c. Molecular mechanisms that govern the lamina-restricted projection of mossy fibers, however, have not been fully understood. We previously studied functions of neural repellent Semaphorin-6A (Sema6A), a class 6 transmembrane semaphorin, and its receptors, plexin-A2 (PlxnA2) and PlxnA4, in mossy fiber projection and have proposed that PlxnA4-expressing mossy fibers are principally prevented from entering the Sema6A-expressing suprapyramidal and infrapyramidal regions of CA3 but are permitted to grow into proximal parts of the regions, where repulsive activity of Sema6A is competitively suppressed by PlxnA2 (Suto et al., 2007). In the present study we demonstrate that Sema6B, another class 6 transmembrane semaphorin, is expressed in CA3 and repels mossy fibers in a PlxnA4-dependent manner *in vitro*. In *Sema6B*-deficient mice several mossy fibers aberrantly project to the stratum radiatum and the stratum oriens. The number of aberrant mossy fibers is increased in *Sema6A;Sema6B* double knock-out mice, indicating that Sema6A and Sema6B function additively to regulate proper projection of mossy fibers. PlxnA2 does not suppress the Sema6B response, but itself promotes growth of mossy fibers. Based on these results, we propose that the balance between mossy fiber repulsion by Sema6A and Sema6B and attraction by PlxnA2 and unknown molecule(s) prescribes the areas permissive for mossy fibers to innervate.

Introduction

In the hippocampus, afferents from various brain regions terminate at specific laminae. In CA3, fibers from the entorhinal cortex terminate at distal parts of the suprapyramidal region [the stratum lacunosum-moleculare (SLM)]; axons from CA3 pyramidal cells of both the contralateral and ipsilateral sides terminate at middle parts of the suprapyramidal region [the stratum radiatum (SR)] and at the stratum oriens (SO) in the infrapyramidal region; and axons of dentate granule cells, mossy fibers, innervate at proximal-most parts of the suprapyramidal region (the stratum lucidum) to form the suprapyramidal bundle and proximal-most parts of the infrapyramidal

region of CA3c to form the infrapyramidal bundle (Amaral and Witter, 1995).

Several attractive and repulsive molecules, such as netrin-1 (Barallobre et al., 2000), RGMA (Brinks et al., 2004), Eph ligand ephrins (Stein et al., 1999; Otal et al., 2006), class 3 semaphorins (Chédotal et al., 1998; Steup et al., 1999, 2000; Cheng et al., 2001; Pozas et al., 2001; Bagri et al., 2003; Liu et al., 2005), Slit-2 (Nguyen-Ba-Charvet et al., 1999), and Reelin (Borrell et al., 2007), and cell adhesion molecules (Cremer et al., 1997; Förster et al., 1998) have been shown to take part in the guidance and termination of hippocampal afferents at proper laminae (for review, see Skutella and Nitsch, 2001). Molecular mechanisms that govern lamina-restricted projection of mossy fibers, however, have not fully been elucidated.

We have previously shown that Semaphorin-6A (Sema6A), a neural repellent of the class 6 transmembrane semaphorin, and its receptors plexin-A2 (PlxnA2) and PlxnA4 play crucial roles in lamina-restricted projection of mossy fibers (Suto et al., 2007). On the basis of projection patterns of mossy fibers in *Sema6A*, *PlxnA2*, *PlxnA4* knock-out mice and double knock-out mice for these genes, we have proposed that mossy fibers express PlxnA4 and are prevented from innervating Sema6A-abundant suprapyramidal and infrapyramidal regions of CA3, but they are permitted to grow into proximal-most parts of these regions, where the repulsive activity of Sema6A is attenuated by PlxnA2 (Suto et al.,

Received Jan. 5, 2010; revised March 17, 2010; accepted April 10, 2010.

This work was supported by Grants-in-Aid from the Ministry of Education, Science, Sports, and Culture of Japan Ministry of Education (H.F.), grants from the 21st Century COE Program (H.T. and H.F.), Grant-in-Aid for Young Scientists (B) and CREST (Core Research for Evolutional Science and Technology) of Japan Science and Technology Agency (F.S.), National Institutes of Health Grant R01 NS065048 (Y.Y.), and a Health Research Board Project Grant (K.J.M.). *Sema6B* mutant mice were generated in, and generously provided by the Dr. T.M. Jessell Laboratory, at Columbia University (New York, NY). We also thank Drs. M. Mendelsohn, J. Kirkland, and B. Han (Columbia University) in the generation of the *Sema6B* mutant mice, and Dr. J. Miyazaki (Osaka University, Suita, Japan) for pCAGGS expression vector.

Correspondence should be addressed to Hajime Fujisawa, Division of Biological Science, Nagoya University Graduate School of Science, Chikusa-ku, Nagoya 464-8602, Japan. E-mail: hcfujisawa@mf.ccnw.ne.jp.

DOI:10.1523/JNEUROSCI.0073-10.2010

Copyright © 2010 the authors 0270-6474/10/307049-12\$15.00/0

2007). On the other hand, the finding that mossy fibers spread into inappropriate laminae of CA3 in *PlxnA4* mutants, while projecting to the normal target lamina in *Sema6A* mutants and *PlxnA2;Sema6A* double mutants (Suto et al., 2007), suggested the existence of additional *PlxnA4*-related mossy fiber repellent(s) in CA3.

We have reported that *Sema6B*, another class 6 semaphorin, repels sympathetic axons and that the repulsive activity of *Sema6B* is mediated by *PlxnA4* (Suto et al., 2005). Here, we report that *Sema6B* is expressed in CA3 and functions as a repellent for mossy fibers. We generate protein-null mutant mice for *Sema6B* and *Sema6A;Sema6B* double knock-out mice and demonstrate that *Sema6B* functions additively with *Sema6A* to regulate proper projection of mossy fibers. In addition, we show that *PlxnA2* does not suppress the *Sema6B* response but itself promotes growth of mossy fibers. Based on the findings obtained in the present and previous studies (Suto et al., 2007), we discuss how *Sema6A* and *Sema6B* and their receptors, *PlxnA2* and *PlxnA4*, work in concert to regulate proper projection of mossy fibers.

Materials and Methods

Generation of mice lacking *Sema6B*. Mouse genomic clones were derived from a 129/Sv genomic library (Stratagene). A targeting vector was constructed using a 9 kb *NotI*-*BglI* (*NotI* is derived from the phage DNA, and *BglI* was added just before the sequences corresponding to the first methionine) fragment and a 3 kb *BamHI*-*Sall* (*Sall* is derived from the phage DNA) fragment. The *LoxP*-*PlxnA4*PGKneo-triple pA signal-*LoxP* cassette and the farnesylated EGFP-pA cassette (where PGK is phosphoglycerate kinase and EGFP is enhanced green fluorescent protein) were inserted between the *NotI*-*BglI* and *BamHI*-*Sall* fragments. A linearized targeting construct was electroporated into 129Sv/Ev-derived embryonic stem (ES) cells. Cells were selected with G418 and screened by Southern blot analysis. Southern blot analysis was done on the *EcoRI* fragments of genomic DNA using a 0.5 kb fragment as a probe (see Fig. 1A) that generates a 14 kb wild-type band and an 8 kb mutant band. The ES cells carrying the correct mutation were injected into C57BL/6J blastocysts. Chimeric offsprings were mated with C57BL/6J mice. Germ line transmission of the mutant allele was determined by Southern blot analysis of genomic DNA from tails of mice. Heterozygous F1 animals were intercrossed to obtain homozygous (*Sema6B*^{-/-}) mice. Genotypes of mice were determined by PCR using the following primers: P1 (5'-CTCACATGTGGTCTTAAAGTCGCTTG-3') and P2 (5'-TGATATCGCAGCTCCGTGGAAGTGG-3') for the wild-type allele and P1 and neo-4 (5'-CCTGATCGACAAGACCGGCTTC-3') within the neomycin resistance gene for the mutant allele (see Fig. 1A). Amplification of DNA was performed using Ex-TaqDNA polymerase (Takara).

Animals. *Sema6A;Sema6B* double knock-out mice and *PlxnA2;Sema6B* double knock-out mice were generated by crossing *Sema6B* mutant mice with *Sema6A* mutant mice (Leighton et al., 2001; Mitchell et al., 2001) and *PlxnA2* mutant mice (Suto et al., 2007), respectively. Noon on the day on which a copulation plug was found was designated as embryonic day 0.5 (E0.5). The day of birth was designated as postnatal day 0 (P0). All animal experiments and animal care were performed along with the guidelines of the Animal Care and Experimentation Committee of each institution.

Immunoblot analysis, histology, and in situ hybridization analysis. Immunoblot analysis using goat anti-human *Sema6B* antibodies (0.2 μg/ml; R & D Systems) was done on the extract of E16.5 mouse embryonic brains following the procedures reported (Shimizu et al., 2000). General procedures for Timm staining and immunohistochemistry have been reported previously (Suto et al., 2007). In this study, rabbit calbindin D-28k antibodies (Swant), rabbit calretinin antibodies (Swant), and an Armenian hamster monoclonal antibody for mouse *PlxnA4* Mab-A4F5 (Suto et al., 2007) were used as primary antibodies. The calbindin and calretinin antibodies were detected by biotinylated anti-rabbit IgG (GE Healthcare) and a Vectastain ABC kit (Vector Laboratories), and the

PlxnA4 antibody was detected by Cy3-conjugated goat anti-Armenian hamster IgG (Jackson ImmunoResearch Laboratories). *In situ* hybridization (ISH) was performed by using the digoxigenin-labeled cRNA that corresponds to 1–833 bases of the mouse *Sema6B* cDNA (GenBank accession no. NM_013662) as a probe, following the procedures reported (Murakami et al., 2001; Suto et al., 2003).

Culture of hippocampal slices. Organotypic culture of hippocampal slices was performed following the procedures reported previously (Mizuhashi et al., 2001; Suto et al., 2007).

Transfection of cultured pyramidal cells. To construct the expression plasmid for myc-tagged full-length *Sema6B* (myc-full-*Sema6B*), the sequences encoding the myc epitope were added at the 3'-end of the signal sequences of the *Sema6B* cDNA. The expression plasmid contained the Kozak-like sequences in the 5'-untranslated region (UTR) and the 3'-UTR (see GenBank accession no. NM_013662). The myc-tagged *Sema6B* cDNA was ligated into an expression vector pCAGGS (pCAGGS-myc-full-*Sema6B*; pCAGGS, a gift from Dr. J. Miyazaki, Osaka University, Suita, Japan). Hippocampal neurons from E16.5 mouse embryos were cultured for 4 d, following the procedures reported (Goslin et al., 1998; Suto et al., 2007), and cotransfected with the pCAGGS-myc-full-*Sema6B* and an EGFP expression plasmid, pEGFP-N1 (Clontech), using Lipofectamine 2000 (Invitrogen). At 24 h after the transfection, cultures were fixed with 4% paraformaldehyde (PFA) and then immunostained with rabbit anti-myc antibody A-14 (Santa Cruz Biotechnology) and a mouse monoclonal antibody for MAP2 HM-2 (Sigma). To detect the antibodies A-14 and HM-2, Alexa Fluor 546-conjugated goat anti-rabbit IgG (Invitrogen) and Alexa Fluor 488-conjugated goat anti-mouse IgG (Invitrogen) were used as secondary antibodies, respectively.

Production of recombinant proteins. To construct the expression plasmids, pCAGGS-*Sema6Bect*-Fc-*His₆* for the Fc-dimerized ectodomain of *Sema6B* (*Sema6Bect*-Fc) and pCAGGS-AP-Fc-*His₆* for Fc-dimerized alkaline phosphatase (AP-Fc), the sequences corresponding to the 26–599 amino acid residues of the mouse *Sema6B* protein and the 38–528 amino acid residues of the human placental alkaline phosphatase protein were inserted into the pCAGGS-*Sema3Ass*-Myc-Fc-*His₆* vector (Suto et al., 2007), respectively. Generation of the expression plasmids pCAGGS-*Sema6Aect*-Fc-*His₆* for the Fc-dimerized ectodomain of *Sema6A* (*Sema6Aect*-Fc) and pCAAGGS-*PlxnA2SD*-Fc-*His₆* for the sema domain of *PlxnA2* (*PlxnA2SD*-Fc) were reported previously (Suto et al., 2007). Human embryonic kidney 293T (HEK293T) cells were transfected with pCAGGS-*Sema6Aect*-Fc-*His₆*, pCAGGS-*Sema6Bect*-Fc-*His₆*, pCAAGGS-*PlxnA2SD*-Fc-*His₆*, or pCAGGS-AP-Fc-*His₆* using Effectene (Qiagen). Recombinant proteins were purified from culture supernatants using Ni-NTA (nickel-nitrilotriacetic) agarose (Qiagen) and dialyzed against Dulbecco's calcium- and magnesium-free PBS for 2 d.

Growth cone collapse assay. Small fragments of the dentate gyrus from P2 mice were cultured with NB/B-27 medium (Invitrogen) in 8-well chamber slides (Nunc) that had been coated with poly-L-lysine (PLL, 100 μg/ml; Sigma) and mouse laminin (10 μg/ml; Invitrogen). On the second day of cultivation, *Sema6Aect*-Fc recombinant proteins or *Sema6Bect*-Fc recombinant proteins were added to the cultures for 1 h at 37°C. The cultures were fixed with PFA and processed for immunohistochemistry with calbindin antibodies to detect mossy fibers.

Competition assay. To examine effects of *PlxnA2* on the *Sema6A*- or *Sema6B*-induced growth cone collapse in mossy fibers, *Sema6Aect*-Fc recombinant proteins or *Sema6Bect*-Fc recombinant proteins (20 nM each) were preincubated with *PlxnA2SD*-Fc recombinant proteins or AP-Fc recombinant proteins (200 nM each) in NB/B-27 medium for 30 min at 37°C. The protein mixtures were then applied to explant cultures of the dentate gyrus to examine their growth cone collapse activities; half volume of the culture medium was replaced with the protein mixtures.

Ligand-absorption assay. To examine interaction of *Sema6A* and *Sema6B* to *PlxnA2* and *PlxnA4*, *Sema6Aect*-Fc recombinant proteins (2 nM) or *Sema6Bect*-Fc recombinant proteins (20 nM) were added to suspension cultures of 1×10^7 *PlxnA2*-expressing L cells (LA2 cells) (Suto et al., 2007), *PlxnA4*-expressing L cells (LA4 cells) (Suto et al., 2003), or parental L cells in 1 ml of NB/B-27 medium and gently agitated for 1 h at

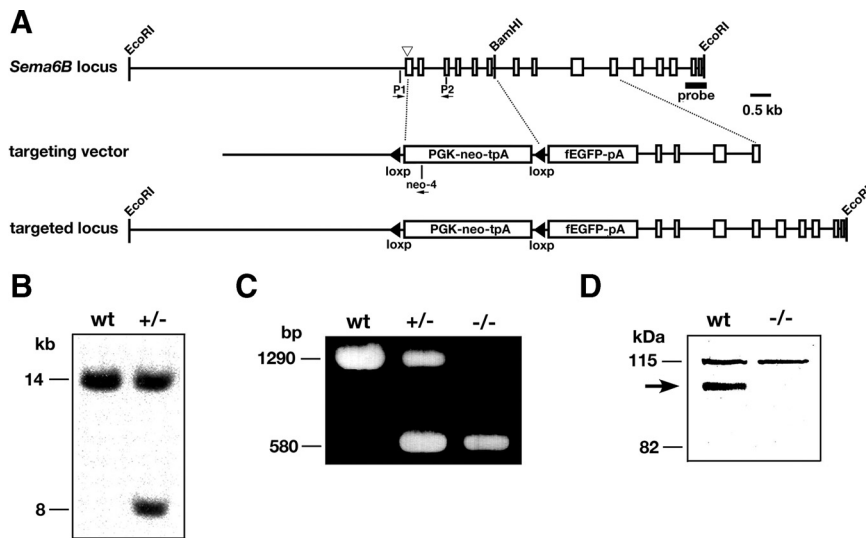


Figure 1. Generation of *Sema6B* mutant mice by targeted disruption of the *Sema6B* gene. **A**, Schematic illustration of the *Sema6B* gene (*Sema6B* locus), the targeting vector, and the targeted locus. Exons are indicated by boxes. The exon 1 in the 5' upstream is omitted in the scheme. ∇ , Position of the initiation codon in the exon 2, ATG; PGK-neo-tpA, PGKneo-triple poly(A) cassette; fEGFP-pA, farnesylated EGFP-poly(A) cassette. **B**, Southern blot analysis on the EcoRI-digested genomic DNA from targeted ES cells, using a 3' external probe (probe in **A**). Note that expected sizes of DNAs, 14 kb for the wild-type (wt) allele and 8 kb for the targeted allele, are detected. **C**, PCR analysis using primers, P1, P2, and neo-4 in **A**. Expected sizes of DNAs, 1.3 kb for the wild-type allele and 0.6 kb for the mutant allele, are amplified in animals derived from *Sema6B* heterozygous intercrosses. **D**, Immunoblot analysis using goat anti-human *Sema6B* antibodies. A band for the *Sema6B* proteins is detected at 100 kDa position (arrow) in the extracts of brains from E16.5 wt but not *Sema6B* homozygous ($-/-$) mouse embryos. A band at 115 kDa position is a nonspecific binding of the antibody.

4°C. The culture supernatants were collected by centrifugation and then applied to explant cultures of the dentate gyrus to examine their growth cone collapse activities; half volume of the culture medium was replaced with the supernatant.

Generation of 3T3 cells that stably express transgenes. NIH3T3 cells were cotransfected with the expression plasmids for myc-tagged full-length mouse *Sema6B* (Suto et al., 2005) or PlxnA2 (Suto et al., 2007) and pST-neoB (Katoh et al., 1987) using Effectene, and selected with Geneticin (700 μ g/ml; Invitrogen). Cell clones that express *Sema6B* (6B/3T3) or PlxnA2 (A2/3T3) were identified with a mouse monoclonal antibody for myc 9E10 (Evan et al., 1985). To isolate cell lines that doubly express PlxnA2 and *Sema6B* (A2::6B/3T3 cells), 6B/3T3 cells were transfected with the PlxnA2 expression plasmid and pCEP4 (Invitrogen), selected by hygromycin B (100 μ g/ml; Roche), and stained with rabbit anti-PlxnA2 antibodies (Suto et al., 2007). 3T3 cells were cultured with DMEM (Sigma) containing 10% fetal bovine serum (JRH Biosciences).

Neurite outgrowth assay. Explants of the dentate gyrus from P2 mouse were cultured for 3 d on monolayer sheets of 6B/3T3 cells, A2/3T3 cells, A2::6B/3T3 cells, or parental 3T3 cells with a medium consisted of 70% DMEM, 15% HBSS, and 15% fetal bovine serum supplemented with B-27 Supplement Minus AO (Invitrogen) and 25 mM D-glucose. On the second day, half volume of the medium was exchanged with fresh one. Some dentate explants were cultured in PLL-coated chamber slides for 2.5 d. The cultures were fixed and immunostained with calbindin antibodies.

Results

Generation of *Sema6B* knock-out mice

Sema6B is expressed in developing hippocampus (see Fig. 3A). Therefore, to address functions of *Sema6B*, we generated *Sema6B* mutant mice by targeted disruption of the gene. Most parts of the exon 2, including the sequences encoding the first methionine, and the exons 3–7 of the *Sema6B* gene were replaced by the PGKneo-poly(A) cassette and the EGFP-poly(A) cassette (Fig. 1) (for details, see Materials and Methods). As the targeted locus lacks the initiation codon and instead contains the poly(A)-

added neomycin-resistant gene and the GFP gene, *Sema6B* homozygous mice (*Sema6B*^{-/-} mice) were expected to be protein null. Immunoblot analysis revealed a band at ~100 kDa position in the brain extracts from E16.5 wild-type but not *Sema6B*^{-/-} embryos (Fig. 1D), indicating that the mutant mice lack the intact *Sema6B* proteins. Homozygous animals were recovered from mating of heterozygous parents at a frequency that was predicted by the laws of Mendelian inheritance, suggesting that the deprivation of *Sema6B* does not affect the viability of the animals. In addition, both male and female homozygous mice were fertile.

Abnormal projection of mossy fibers in *Sema6B* mutant mice

We first examined projection patterns of mossy fibers in adult *Sema6B* mutant mice by Timm staining and calbindin immunohistochemistry, which can visualize presynaptic terminals and trajectories of mossy fibers, respectively. In *Sema6B* homozygous (*Sema6B*^{-/-}) mice ($n = 10$), projection of mossy fibers was abnormal in several points. As in wild-type mice (Fig. 2A,I), mossy fibers in *Sema6B* mutant mice innervated into proximal parts of the suprapyramidal and infrapyramidal regions of CA3 and formed the suprapyramidal and infrapyramidal bundles, respectively (Fig. 2E,J). However, the suprapyramidal bundle was thicker and the infrapyramidal bundle was longer in *Sema6B* mutants than in wild-type animals (Fig. 2, compare A, E; also see Fig. 7H). Several Timm-positive spots were observed in SR and SO of CA3ab in the mutants but not wild-type animals (Fig. 2, compare G, H, C, D), indicating inappropriate spreading of mossy fibers from the suprapyramidal and infrapyramidal bundles into SR and SO. In addition, several mossy fibers directly invaded SR and SO of CA3c without forming the suprapyramidal or infrapyramidal bundles (Fig. 2F,J). These results indicate that *Sema6B* plays roles in proper projection of mossy fibers.

It has been reported that the first mossy fibers invade CA3 at around P0, and their number gradually increases during postnatal development (Amaral and Dent, 1981). As *Sema6B* is expressed in the hippocampus of neonatal mice (see Fig. 3A), we examined whether deficiency of *Sema6B* induces abnormal projection of mossy fibers in early postnatal stages. Timm staining, calbindin immunohistochemistry, or dye filling of mossy fibers in P5 and P10 *Sema6B*^{-/-} mice, however, did not successfully demonstrate abnormal projection of the fibers, probably because of the small number of aberrant mossy fibers. On the other hand, cultures of hippocampal slices from P5 *Sema6B*^{-/-} mice for 5 d demonstrated obvious abnormality in mossy fiber projection. In the hippocampal slices from wild-type animals ($n = 22$), mossy fibers terminated exclusively at proximal parts of the suprapyramidal region to form a tightly packed suprapyramidal bundle (Fig. 2K). In contrast, in the hippocampal slices from *Sema6B* mutants ($n = 18$), mossy fibers formed a very thin suprapyramidal bundle and, instead, spread widely within SR (Fig. 2L). These results indicate that *Sema6B* is required for proper projection of mossy fibers from the beginning of its development.

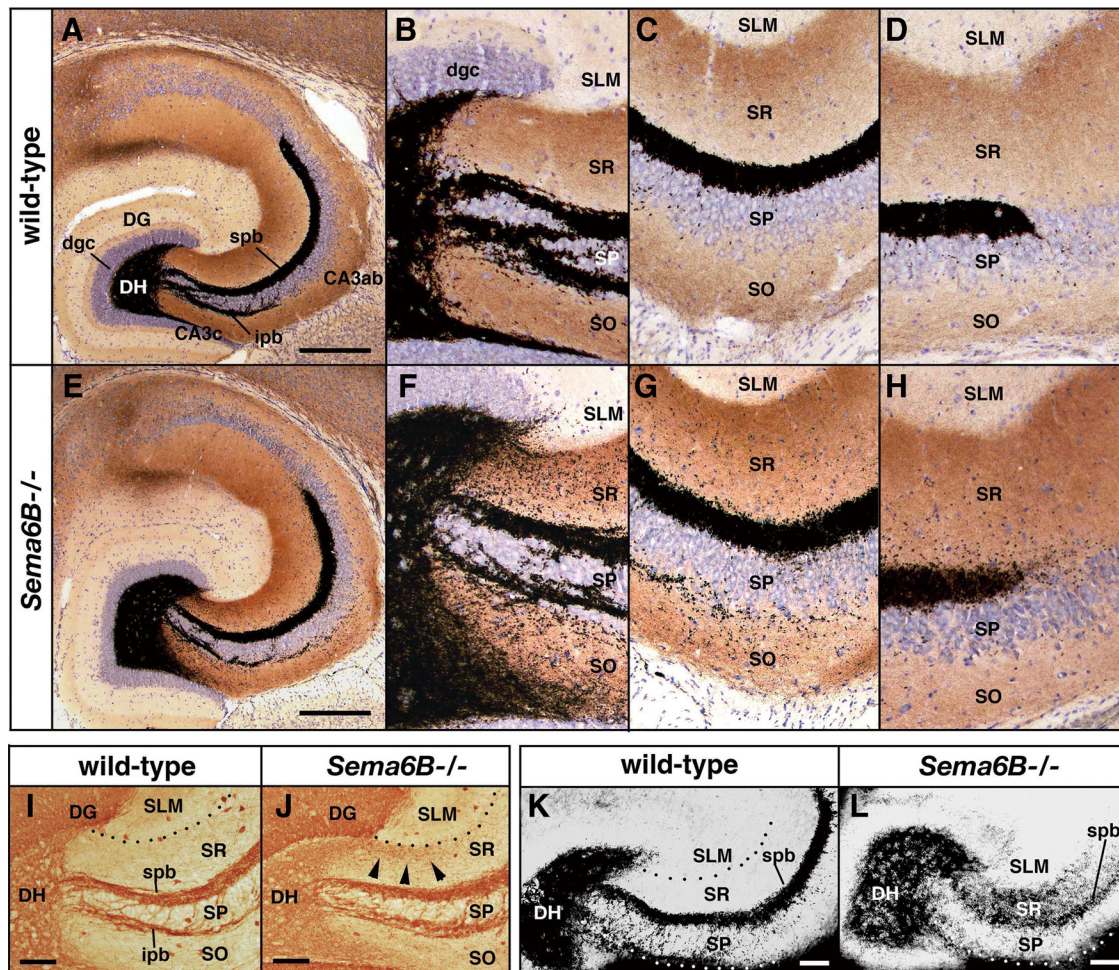


Figure 2. Mossy fiber projection in *Sema6B* mutant mice. **A–J**, Timm staining (**A–H**) and immunostaining with calbindin (**I, J**) of horizontal sections of the hippocampus of adult wild-type and *Sema6B* homozygous (*Sema6B*^{-/-}) mice. The regions corresponding to CA3c, the middle part of CA3ab, and the distal-most part of CA3ab in **A** and **E** are shown at a higher magnification in **B–D** and **F–H**, respectively. Arrowheads in **J** indicate mossy fibers that directly grow into the SR. DG, Dentate gyrus; DH, dentate hilus; SL, stratum lucidum; dgc, dentate granule cell; spb, suprapyramidal bundle of mossy fibers; ipb, infrapyramidal bundle of mossy fibers. These abbreviations also apply to other figures of this article. **K, L**, Timm staining of hippocampal slices from P5 wild-type and *Sema6B*^{-/-} mice that were cultured for 5 d. Scale bars: **A, E**, 400 μ m; **I–L**, 100 μ m.

Expression of Sema6B in CA3 pyramidal cells is essential for proper projection of mossy fibers

In situ hybridization analysis revealed that expression of Sema6B was prominent in CA3 pyramidal cells of neonatal mice in which mossy fibers are vigorously growing into CA3 (Fig. 3A). Sema6B was also expressed in dentate granule cells, raising a question as to whether Sema6B in CA3 pyramidal cells and/or dentate granule cells is essential for proper projection of mossy fibers. To address this question, we prepared slices of the dentate gyrus and CA3 from P5 wild-type and *Sema6B*^{-/-} mice, cocultured them in various combinations (Fig. 3B) for 5 d, and then examined projection patterns of mossy fibers.

In cocultures of CA3 slices from wild-type mice with dentate gyrus slices from wild-type mice ($n = 18$) (Fig. 3C) or *Sema6B*^{-/-} mice ($n = 20$) (Fig. 3E), mossy fibers projected to proximal-most parts of the suprapyramidal region of CA3, the normal projection sites for the fibers. In contrast, when CA3 slices from *Sema6B*^{-/-} mice were cocultured with dentate gyrus slices from wild-type mice ($n = 19$) (Fig. 3D) or *Sema6B*^{-/-} mice ($n = 23$) (Fig. 3F), mossy fibers abnormally spread into SR, as observed in the hippocampal slices from *Sema6B*^{-/-} mice (see Fig. 2L). These results indicate that Sema6B in CA3 pyramidal cells plays a primal role in proper projection of mossy fibers.

We next addressed the question of the subcellular localization of Sema6B proteins in pyramidal cells. All Sema6B antibodies tested were not usable for immunohistochemistry. We therefore transfected cultured hippocampal neurons with an expression plasmid for myc-tagged full-length Sema6B and found that the exogenous Sema6B proteins were localized on dendrite-like but not axon-like cell processes (supplemental Fig. 1, available at www.jneurosci.org as supplemental material). The result suggests that the Sema6B proteins exist on dendrites of pyramidal cells *in vivo*.

Sema6B is a repellent for mossy fibers

The abnormal innervation of mossy fibers into SR and SO in *Sema6B*-deficient mice raises a possibility that Sema6B functions as a repellent for mossy fibers to prohibit innervation of the fibers into the laminae. To test the possibility, we investigated whether Sema6B can collapse growth cones of mossy fibers. Figure 4, A and C, shows that recombinant proteins for the Fc-dimerized Sema6B ectodomain Sema6Bect-Fc collapsed growth cones of mossy fibers from wild-type animals in a dose-dependent manner. In contrast, the recombinant proteins did not collapse growth cones of mossy fibers from *PlxnA4* homozygous (*PlxnA4*^{-/-}) mice (Fig. 4B,C).

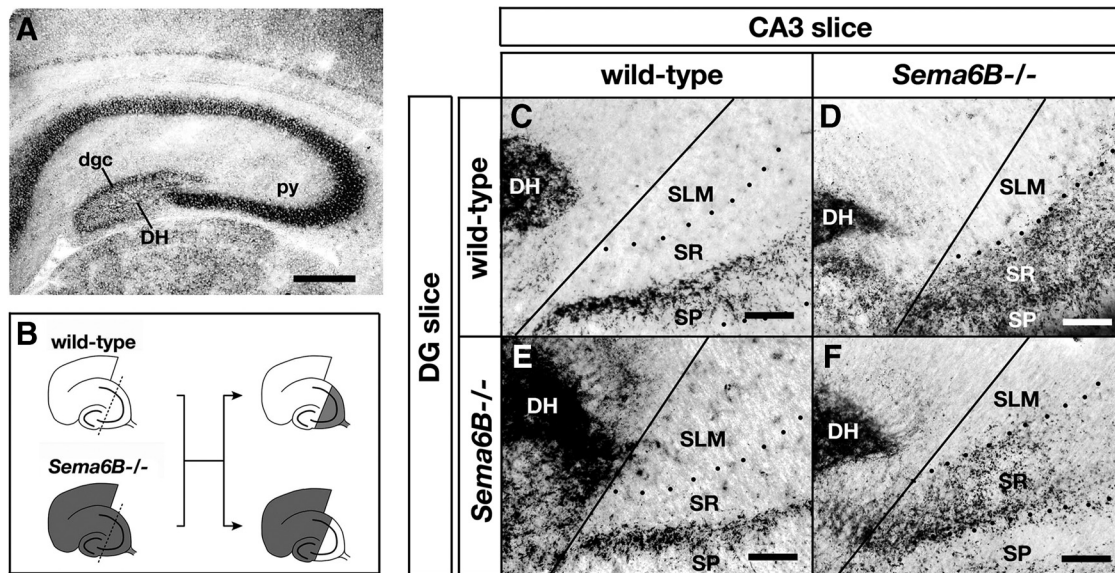


Figure 3. Expression of Sema6B and mossy fiber projection in chimeric cocultures of hippocampal slices. **A**, Expression of *Sema6B* in the hippocampus of P5 mice detected by ISH analysis. Note a strong ISH signal in pyramidal cells (py). **B**, Schematic diagram of the chimeric coculture. Horizontal slices of the hippocampus of P5 wild-type and *Sema6B*^{-/-} mice are divided into two pieces; a slice that contains the dentate gyrus (DG slice) and a slice that contains CA3 (CA3 slice). The DG slices and the CA3 slices were combined in various combinations and cultured for 5 d. **C–F**, Timm staining of the cocultures. Solid lines indicate the border of the DG slice and CA3 slice. Dotted lines indicate the boundary between SLM and SR in **C–F** and also SR and SP in **F**. Scale bars: **A**, 200 μm ; **C–F**, 100 μm .

We further investigated whether Sema6B suppresses growth of mossy fibers. We cultured explants of the dentate gyrus from P2 mice on monolayer sheets of NIH3T3 cells (3T3 cells) or 3T3 cells that stably expressed the full-length mouse Sema6B proteins (6B/3T3 cells). Outgrowth of mossy fibers from wild-type dentate explants vigorously occurred on 3T3 cells (Fig. 4D) but was suppressed on 6B/3T3 cells (Fig. 4F); average length of mossy fibers on 6B/3T3 cells was $104 \pm 3 \mu\text{m}$ and was less than one-third of that on 3T3 cells ($378 \pm 11 \mu\text{m}$) (Fig. 4H). In contrast, mossy fibers from *PlxnA4*-deficient dentate explants sprouted well on both 3T3 cells and 6B/3T3 cells (Fig. 4E,G,H).

Taken collectively, the results obtained by the growth cone collapse assay and the neurite outgrowth assay indicate that Sema6B functions as a repellent for mossy fibers and, furthermore, that the repulsive activity of the semaphorin is mediated by *PlxnA4*.

Sema6A and Sema6B additively suppress aberrant projection of mossy fibers

Our previous study has shown that *Sema6A* mutant mice do not show any obvious abnormality in mossy fiber projection, although Sema6A functions as a potent repellent for mossy fibers *in vitro* (Suto et al., 2007), raising a possibility that activities of Sema6A are compensated by Sema6B. We therefore examined projection patterns of mossy fibers in *Sema6A*;*Sema6B* double knock-out mice. In *Sema6A*;*Sema6B* double homozygous mice (*Sema6A*^{-/-};*Sema6B*^{-/-} mice; $n = 8$), the suprapyramidal bundle was thicker and the infrapyramidal bundle was longer than in *Sema6B* mutant mice (compare Figs. 5A–D, 2E–H). More mossy fibers aberrantly spread into SR and SO of CA3ab in the *Sema6A*;*Sema6B* double mutants than in *Sema6B* mutants (compare Figs. 5C,D, 2G,H). In addition, number of mossy fibers that directly grew into SR and SO of CA3c increased in the double mutants (Fig. 5B). These results indicate that not only Sema6B but also Sema6A function as mossy fiber repellents to suppress aberrant spreading of mossy fibers into SR and SO.

Repulsive activities of both Sema6A and Sema6B are mediated by *PlxnA4*. Therefore, we had initially expected that projection patterns of mossy fibers in *Sema6A*;*Sema6B* double mutants would be closely related to those in *PlxnA4* mutants. Mossy fiber phenotypes, however, were different between these two mutant mouse lines; mossy fibers aberrantly spread into SR and SO, but not SLM, in *Sema6A*;*Sema6B* double mutants, but into SR, SO, and SLM in *PlxnA4* mutants (Suto et al., 2007) (Fig. 5E). These findings suggest the existence of additional *PlxnA4*-related mossy fiber repellent(s) in SLM.

We noted an additional defect in the projection of mossy fibers in these mutants. Mossy fibers do not normally invade the molecular layer of the dentate gyrus (Fig. 5F). In *Sema6B* mutants, however, a few Timm-positive spots were detected in the inner third of the molecular layer, the inner molecular layer, which is a target lamina for axons of mossy cells located in the dentate hilus (Fig. 5G). Aberrant projection of mossy fibers to the inner molecular layer was more prominent in *Sema6A*;*Sema6B* double mutants than in *Sema6B* mutants (Fig. 5, compare H, G), although mossy fibers did not ectopically project to the molecular layer in *Sema6A* single mutants (data not shown). On the other hand, in *PlxnA4* mutants several Timm-positive spots were detected not only in the inner molecular layer but also the outer molecular layer that normally receives fibers from the entorhinal cortex (Fig. 5I). These results indicate that Sema6A and Sema6B also serve as repellents for mossy fibers in the dentate gyrus to prevent abnormal projection of the fibers into the molecular layer and, furthermore, that the outer molecular layer contains other *PlxnA4*-related repellent(s) for mossy fibers.

ISH signals for the *PlxnA4* transcripts were detected in cells of the dentate hilus, and the *PlxnA4* proteins were observed in the inner molecular layer (Suto et al., 2007) (supplemental Fig. 2, available at www.jneurosci.org as supplemental material), suggesting that mossy cells express *PlxnA4*. We therefore examined projection patterns of mossy cell axons in the mutant mice by immunohistochemistry with antibodies against calretinin, a

marker for mossy cells (Fig. 5J). In *Sema6A* and *Sema6B* mutants, calretinin-positive mossy cell axons slightly spread into the outer molecular layer, the incorrect target lamina for these axons (supplemental Fig. 3, available at www.jneurosci.org as supplemental material). Ectopic spreading of mossy cell axons into the outer molecular layer was prominent in *Sema6A*;*Sema6B* double mutants, though the majority of mossy cell axons remained at their normal target sites to form a discrete lamina, the inner molecular layer (Fig. 5K). In contrast, in *PlxnA4* mutants most mossy cell axons spread into the outer molecular layer and, thereby, the original inner molecular layer completely disappeared (Fig. 5L). These results indicate that *Sema6A*, *Sema6B*, and unknown *PlxnA4*-related repellent(s) in the outer molecular layer also play roles in lamina-restricted projection of mossy cell axons.

PlxnA2 does not attenuate the repulsive activity of *Sema6B* but itself promotes growth of mossy fibers

We have previously shown that *Sema6A* binds to both *PlxnA2* and *PlxnA4* with approximately equal affinity and proposed that *PlxnA2* would competitively suppress binding of *Sema6A* to *PlxnA4* and thereby attenuate the *Sema6A* response on mossy fibers (Suto et al., 2007). As *Sema6B* also binds to *PlxnA2* (Toyofuku et al., 2008), we tested whether *PlxnA2* can attenuate the *Sema6B* response by using the growth cone collapse assay and the neurite outgrowth assay.

To examine the effects of *PlxnA2* on the growth cone collapse activity of *Sema6B*, recombinant proteins for *Sema6B* (*Sema6Bect-Fc*) or *Sema6A* (*Sema6Aect-Fc*) were first incubated with Fc-dimerized recombinant proteins for the sema domain of *PlxnA2* (*PlxnA2SD-Fc*) or the human alkaline phosphatase (*AP-Fc*) for 30 min and then added to the explant cultures of the dentate gyrus (for details, see Materials and Methods). Preincubation of *Sema6A* with *PlxnA2* sema domain significantly reduced the *Sema6A*-induced growth cone collapse (Fig. 6A), confirming our previous study (Suto et al., 2007). In contrast, preincubation of *Sema6B* with *PlxnA2* sema domain did not affect on the growth cone collapse activity of the semaphorin.

The above results suggest that *PlxnA2* does not competitively suppress binding of *Sema6B* to *PlxnA4* and thereby fails to attenuate the *Sema6B* response. The results, however, do not exclude a possibility that the sema domain is insufficient to evoke a strong binding of *Sema6B* to *PlxnA2*. Therefore, we examined whether *Sema6B* binds to the full-length *PlxnA2* and *PlxnA4* with comparable affinities. As the K_d values for the interaction of *Sema6B* with *PlxnA2* or *PlxnA4* were not determined (Suto et al., 2005) (our unpublished observations), we performed the absorption

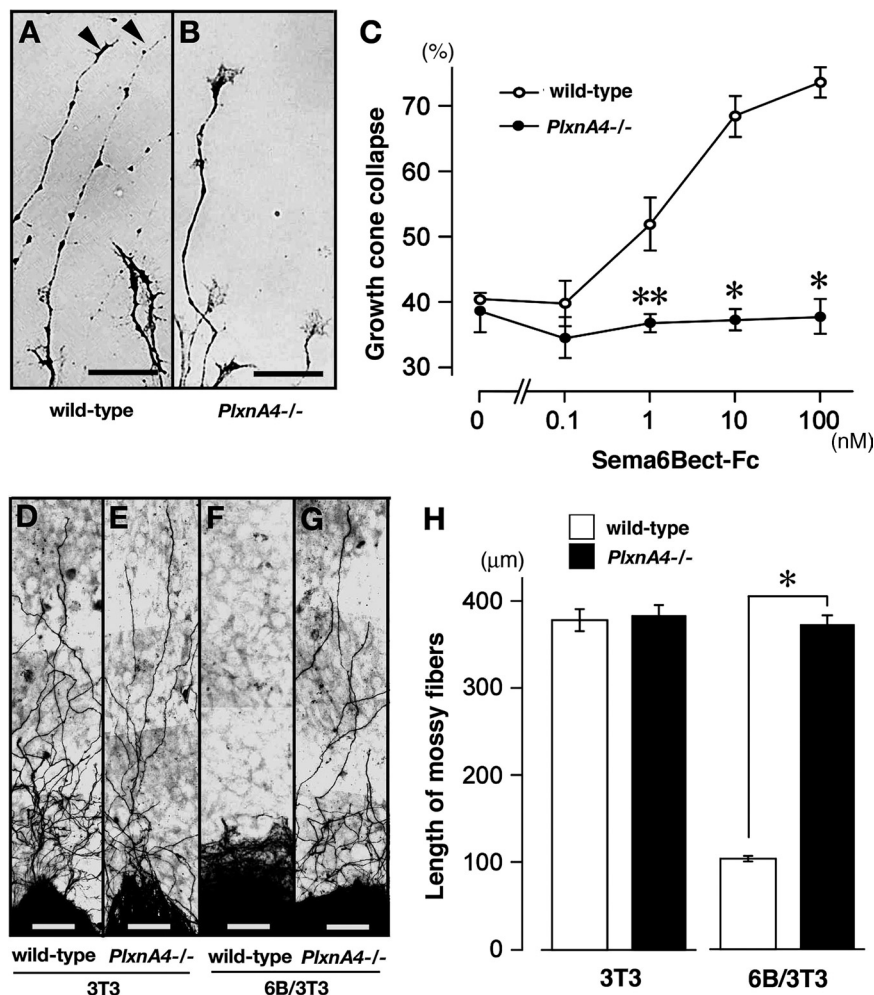


Figure 4. Effects of *Sema6B* on cultured mossy fibers. **A–C**, Collapse of growth cones by *Sema6B*. Explants of the dentate gyrus from P2 wild-type and *PlxnA4* homozygous (*PlxnA4*^{-/-}) mice were cultured for 2 d and then treated with the Fc-dimerized *Sema6B* ectodomain *Sema6Bect-Fc* (100 nM) for 1 h. Mossy fibers were visualized with calbindin antibodies. Note that *Sema6B* induces collapse of growth cones in wild-type mossy fibers (**A**, arrowheads) but not *PlxnA4*-deficient ones (**B**). Incidence of collapsed growth cones was plotted against different concentration of *Sema6B* (**C**). The protein concentration for *Sema6Bect-Fc* was converted as a monomer. The average percentage for growth cone collapse was calculated for five littermates (>60 growth cones at each point for each mouse). **D–H**, Suppression of mossy fiber outgrowth by *Sema6B*. Explants of the dentate gyrus from P2 wild-type mice (**D**, **F**) or *PlxnA4*^{-/-} mice (**E**, **G**) were cultured on monolayer sheets of 3T3 cells (**D**, **E**, 3T3) or *Sema6B*-expressing 3T3 cells (**F**, **G**, 6B/3T3) for 3 d and stained with calbindin antibodies. The average length of mossy fibers is given in **H**. The average length for the longest two mossy fibers for each dentate explant was designated as the length of mossy fibers for the given explant. The length of mossy fibers was determined for >10 explants for each mouse (from five littermates). Vertical bars indicate SEM; * $p < 0.001$; ** $p < 0.005$ (Student's *t* test). Scale bars: **A**, **B**, 10 μm; **D–G**, 50 μm.

test. *Sema6Bect-Fc* or *Sema6Aect-Fc* recombinant proteins were first absorbed with L cells that expressed full-length *PlxnA2* (LA2 cells) or *PlxnA4* (LA4 cells), and then their growth cone collapse activities were examined (for details, see Materials and Methods). Preabsorption of *Sema6A* with either LA2 cells or LA4 cells significantly reduced the growth cone collapse activity of *Sema6A* (Fig. 6B). On the other hand, preabsorption of *Sema6B* with LA2 cells did not affect the growth cone collapse activity of *Sema6B*, although preabsorption with LA4 cells significantly reduced the *Sema6B* response. These results suggest that the affinity between *PlxnA2* and *Sema6B* is too low to interfere with the *PlxnA4*-mediated growth cone collapse activity of *Sema6B*.

We further examined whether *PlxnA2* interferes with the *Sema6B*-induced suppression of mossy fiber outgrowth. We cultured explants of the dentate gyrus on monolayer sheets of 6B/

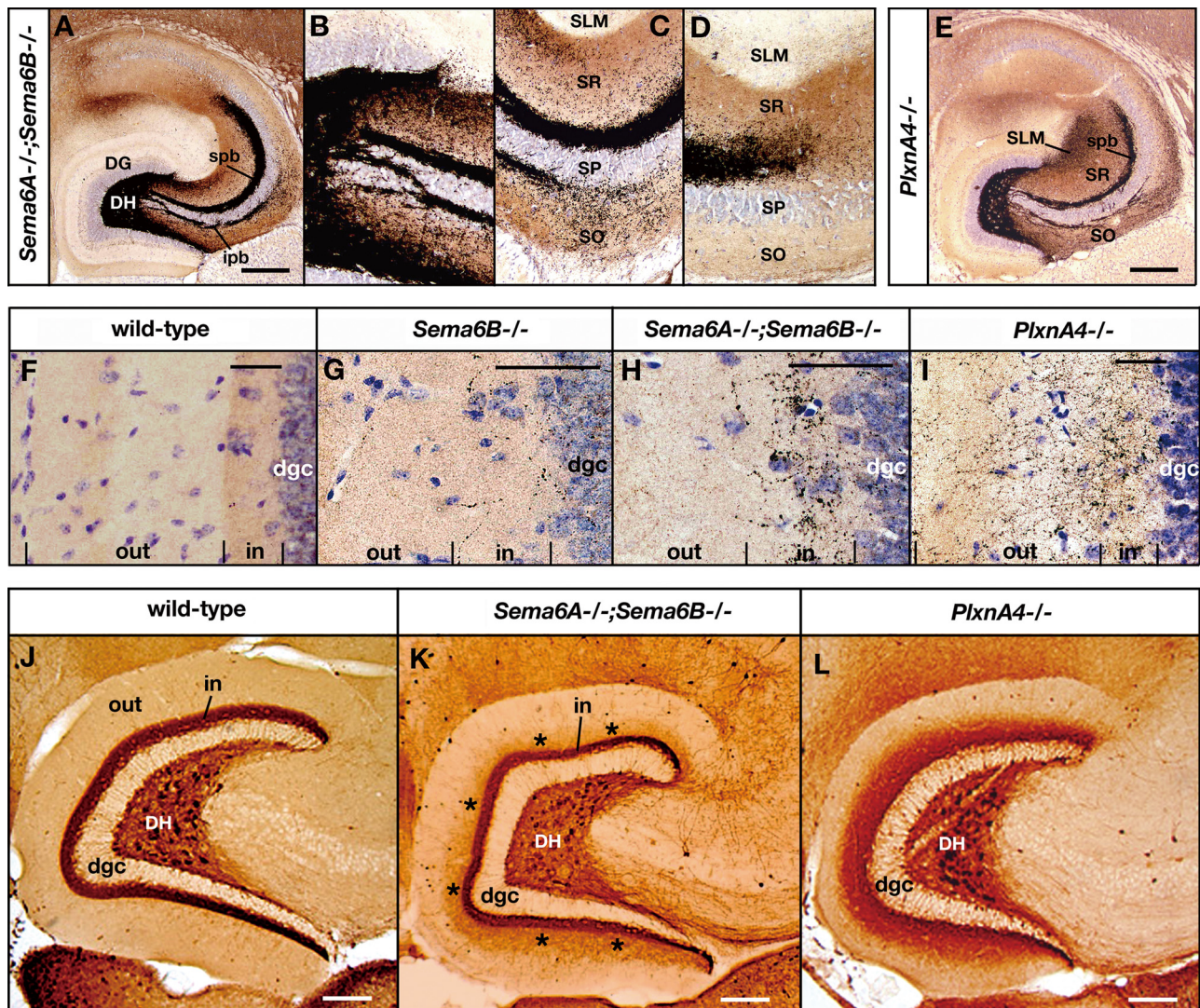


Figure 5. Abnormal projection of mossy fibers and mossy cell axons in *Sema6A*;*Sema6B* double knock-out mice and *PlxnA4* mutant mice. **A–D**, Timm staining of a horizontal section of the hippocampus of an adult *Sema6A*^{-/-};*Sema6B*^{-/-} mouse. The regions corresponding to CA3c, the middle part of CA3ab, and the distal-most part of CA3ab in **A** are shown at a higher magnification in **B–D**. **E**, Timm staining of a horizontal section of the hippocampus of an adult *PlxnA4*^{-/-} mouse. **F–I**, Timm staining of horizontal sections of the dentate molecular layer of adult wild-type and mutant mice. out, Outer molecular layer; in, inner molecular layer. **J–L**, Calretinin immunohistochemistry of horizontal sections of the dentate gyrus of adult wild-type and mutant mice. Note that calretinin-positive mossy cell axons spread ectopically into the outer molecular layer in *Sema6A*;*Sema6B* double mutants (**K**, asterisks) and *PlxnA4* mutants (**L**). Scale bars: **A**, **E**, 400 μ m; **F–I**, 50 μ m; **J–L**, 200 μ m.

3T3 cells or A2::6B/3T3 cells in which the full-length PlxnA2 was coexpressed with Sema6B. To our surprise, the coexpression of PlxnA2 with Sema6B mitigated the Sema6B-induced suppression of mossy fiber outgrowth (Fig. 6C). Furthermore, mossy fibers grew longer on PlxnA2-expressing A2/3T3 cells than parental 3T3 cells. Addition of recombinant proteins for the PlxnA2 sema domain to the dentate explant cultures also enhanced outgrowth of mossy fibers on 3T3 cells, 6B3T3 cells, and PLL-coated culture plates (Fig. 6D). These results indicate that PlxnA2 itself promotes growth of mossy fibers.

Roles of Sema6A, Sema6B, and PlxnA2 in the formation of the suprapyramidal bundle

To evaluate further functions of Sema6A, Sema6B, and PlxnA2 in lamina-restricted projection of mossy fibers, we compared the thickness of the suprapyramidal bundle among *Sema6A*, *Sema6B*, and *PlxnA2* mutant mice and double knock-out mice for these genes.

We first describe projection patterns of mossy fibers in *PlxnA2*;*Sema6B* double knock-out mice. As reported previously (Suto et al., 2007), Figure 7G shows that mossy fibers in *PlxnA2* homozygous (*PlxnA2*^{-/-}) mice terminated at proximal parts of the infrapyramidal region and stratum pyramidalis (SP), but never innervated into the suprapyramidal region. In contrast, in *PlxnA2*;*Sema6B* double homozygous mice (*PlxnA2*^{-/-};*Sema6B*^{-/-} mice; $n = 6$), mossy fibers initially grew into proximal parts of the infrapyramidal region and SP of CA3c, but eventually invaded proximal parts of the suprapyramidal region of CA3ab to form the suprapyramidal bundle (Fig. 7A–D). The suprapyramidal bundle, however, was thinner than that of wild-type animals (compare Figs. 7A, 2A) (Fig. 7H). Furthermore, spreading of mossy fibers from the suprapyramidal and infrapyramidal bundles into SR or SO of CA3ab, which is a typical phenotype in *Sema6B* mutants, did not occur in the *PlxnA2*;*Sema6B* double mutants (Fig. 7C,D), although some mossy fibers directly invaded SR and SO of CA3c (Fig. 7B). In *PlxnA2*;*Sema6B* double

mutants, mossy fibers sometimes grew into SP of CA1 (Fig. 7A). Projection patterns of mossy fibers in *PlxnA2*^{-/-}; *Sema6B*^{+/-} mice ($n = 5$) were closely related to those in *PlxnA2*^{-/-} mutant mice; mossy fibers were restricted to proximal parts of the infrapyramidal region and SP in most parts of CA3, except distal parts of CA3ab, where some mossy fibers grew into the suprapyramidal region and formed a very thin suprapyramidal bundle (Fig. 7F). Projection patterns of mossy fibers in *PlxnA2*^{+/-}; *Sema6B*^{-/-} mice ($n = 5$) were similar to those in *Sema6B*^{-/-} mice (data not shown). The results suggest that *Sema6B* suppresses innervation of mossy fibers into the suprapyramidal region, depending on the dosage of the *Sema6B* gene.

Next, to quantify projection areas for mossy fibers in the suprapyramidal region, we measured the thickness of the suprapyramidal bundle within CA3ab at the position 350 μm from the CA3-CA1 boundary in the *semaphorin* and *plexin* mutant mouse lines. We have previously reported that projection of mossy fibers is mostly normal in *Sema6A* mutants and *PlxnA2*; *Sema6A* double mutants (Suto et al., 2007). The present numerical analysis revealed that the thickness of the suprapyramidal bundles was not significantly different between *Sema6A* mutants and wild-type animals. The suprapyramidal bundle of *PlxnA2*; *Sema6A* double mutants, however, was slightly thinner than that of wild-type animals ($p < 0.01$). The suprapyramidal bundle of *PlxnA2*; *Sema6B* double mutants was thinner than that of wild-type animals ($p < 0.005$) and also *PlxnA2*; *Sema6A* double mutants ($p < 0.01$), indicating that, in the absence of *PlxnA2*, *Sema6A* is a more potent repellent for mossy fibers than *Sema6B* to suppress innervation of the fibers into the suprapyramidal region. On the other hand, the suprapyramidal bundle of *Sema6B* mutants was significantly thicker than that of *Sema6A* mutants ($p < 0.001$) and wild-type animals ($p < 0.001$). These results suggest that mossy fiber repulsion by *Sema6A* but not *Sema6B* is attenuated by *PlxnA2*, resulting in the aberrant spreading of mossy fibers in *Sema6B* but not *Sema6A* mutants. Thickness of the suprapyramidal bundle of *Sema6A*; *Sema6B* double mutants was not exactly determined because of vigorous sprouting of mossy fibers into SR (Fig. 5C,D). However, it is obvious that the suprapyramidal bundle of the double mutants is thicker than that of *Sema6B* mutants.

Discussion

Sema6A, *Sema6B*, and other *PlxnA4*-related repellent(s) regulate proper projection of mossy fibers

This study has shown that *Sema6B*, a member of class 6 semaphorin, collapses growth cones in *PlxnA4*-expressing mossy fibers and suppresses outgrowth of the fibers *in vitro* and,

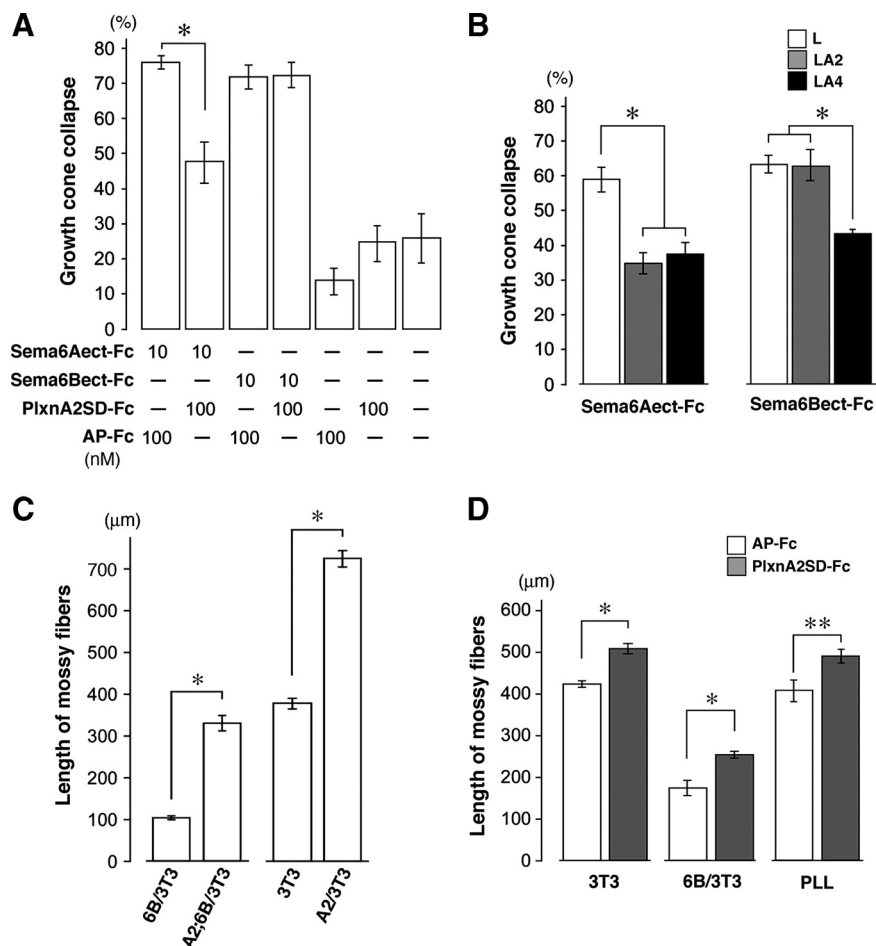


Figure 6. Effects of *PlxnA2* on the *Sema6* response. **A**, Effects of *PlxnA2* sema domain on *Sema6A*-induced and *Sema6B*-induced growth cone collapse in mossy fibers. Recombinant proteins for *Sema6A* (*Sema6Aect-Fc*) or *Sema6B* (*Sema6Bect-Fc*) were preincubated with *PlxnA2* sema domain (*PlxnA2SD-Fc*) or alkaline phosphatase (*AP-Fc*) (see Materials and Methods) and then applied to the explant cultures of the dentate gyrus from P2 mice. **B**, Effects of *PlxnA2* on *Sema6A*-induced and *Sema6B*-induced growth cone collapse in mossy fibers. *Sema6A* (*Sema6Aect-Fc*) and *Sema6B* (*Sema6Bect-Fc*) were preabsorbed by L cells (L), *PlxnA2*-expressing L cells (LA2), or *PlxnA4*-expressing L cells (LA4) and then applied to the cultures. In **A**, **B** the average percentages in growth cone collapse were calculated for five independent experiments. **C**, Effects of *PlxnA2* on mossy fiber outgrowth. Explants of the dentate gyrus from P2 wild-type mice were cultured on monolayer sheets of 3T3 cells, *Sema6B*-expressing cells (6B/3T3 cells), *PlxnA2*-expressing cells (A2/3T3), or cells that coexpress *PlxnA2* and *Sema6B* (A2::6B/3T3). Data for the explant culture on 3T3 cells and 6B/3T3 cells are same as those in Fig. 4H. **D**, Effects of the *PlxnA2* sema domain on mossy fiber outgrowth. Explants of the dentate gyrus were cultured on monolayer sheets of 3T3 cells, 6B/3T3 cells, or PLL-coated culture plates under the presence of *PlxnA2SD-Fc* (100 nM) or *AP-Fc* (100 nM). The average length of mossy fibers was calculated for five independent experiments. Vertical bars indicate SEM; * $p < 0.001$, ** $p < 0.01$ (Student's *t* test).

furthermore, that *Sema6B* deficiency in mice induces spreading of mossy fibers into incorrect target laminae within CA3. These results indicate that *Sema6B* signals via *PlxnA4* function as repellents for mossy fibers (Fig. 8A) and play crucial roles in proper projection of the fibers.

We have previously shown that signals of *Sema6A*, another member of class 6 semaphorin, are also mediated by *PlxnA4* and repel mossy fibers (Suto et al., 2007) (Fig. 8A). The *Sema6A* response, however, is attenuated by *PlxnA2* (Suto et al., 2007) (Fig. 8A), and therefore *Sema6A*-deficient mice do not show any abnormality in mossy fiber projection (Suto et al., 2007). The lack of mossy fiber phenotype in *Sema6A* mutants has raised a question for the function of *Sema6A* in mossy fiber projection. This study has revealed that more aberrant mossy fibers are induced in *Sema6A*; *Sema6B* double mutants than in *Sema6B* mutants (Fig. 8B) and, furthermore, that *PlxnA2*; *Sema6B* double mutants in which *PlxnA2* is deprived, thereby allowing the repulsive activi-

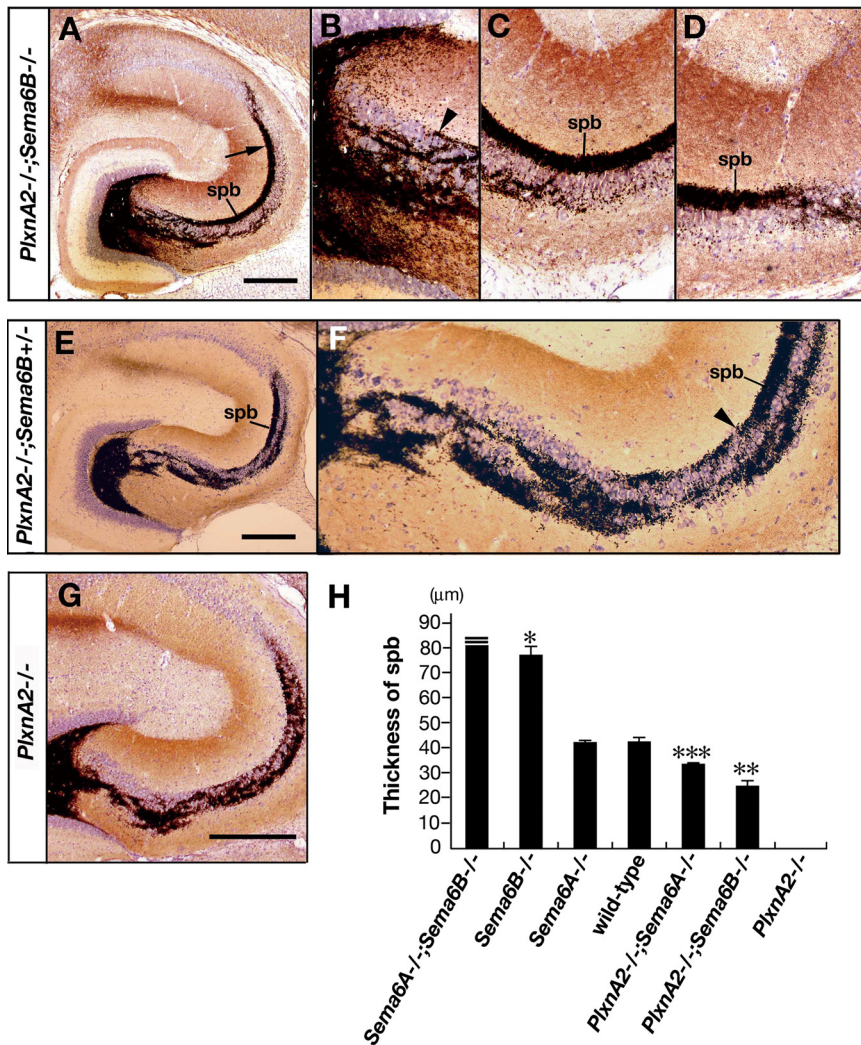


Figure 7. Formation of the suprapyramidal bundle (spb) in *semaphorin* and *plixin* mutant mice. **A–G**, Timm staining of horizontal sections of the hippocampus of adult *PlxnA2*^{-/-};*Sema6B*^{-/-} mice (**A–D**), *PlxnA2*^{-/-};*Sema6B*^{+/-} mice (**E, F**), and *PlxnA2*^{-/-} mice (**G**). The regions corresponding to CA3c, the middle part of CA3ab, and the distal-most part of CA3ab in **A** and **E** are shown at a higher magnification in **B–D** and **F**, respectively. Arrowheads in **B** and **F** indicate the positions where mossy fibers first innervated into the suprapyramidal region to form the suprapyramidal bundle. **H**, Thickness of the spb in adult mice. Thickness of the suprapyramidal bundle was determined within CA3ab at the position 350 μm from the CA3–CA1 boundary (**A**, arrow), for >15 horizontal sections of each mouse (from five mice for each line). *PlxnA2* mutant mice lack the suprapyramidal bundle. Vertical bars indicate SEM; **p* < 0.001, ***p* < 0.005, and ****p* < 0.01 against wild-type mice (Student's *t* test). Scale bars: **A, E, G**, 400 μm.

ties of *Sema6A* to remain intact, exhibit a significant reduction in mossy fiber innervation into the suprapyramidal region (Fig. 8B). We therefore conclude that repulsive activities of *Sema6A* also play a practical role in proper projection of mossy fibers. The *PlxnA2* proteins are distributed in a proximodistal gradient within the suprapyramidal region (Suto et al., 2007). Therefore, the *Sema6A* response would be completely attenuated in proximal-most parts of the suprapyramidal region, resulting in a mossy fiber phenotype in wild-type animals similar to that in *Sema6A* mutants. On the other hand, in distal parts of the suprapyramidal region the *Sema6A* response would be suppressed but not attenuated completely by *PlxnA2*. This may cause the wider spreading of mossy fibers in *Sema6A*;*Sema6B* double mutants than in *Sema6B* mutants.

This study has shown that the abnormal projection of mossy fibers in *Sema6B* mutants is due to the deficiency of *Sema6B* in CA3 pyramidal cells but not mossy fibers. The present transfect-

ion study suggests that *Sema6B* exists on dendrites of pyramidal cells and prevents innervation of mossy fibers into the suprapyramidal and infrapyramidal regions where pyramidal cell dendrites are distributed. The transfection study, however, cannot completely rule out the possibility that *Sema6B* exists on axons of pyramidal cell. *Sema6A* exists on both dendrites and axons of pyramidal cells (Suto et al., 2007). Kapfhammer and Raper (1987a,b) have reported repulsive interaction between different fiber classes. Therefore, it is also possible that axons of pyramidal cells in SR and SO, the commissural/associational fibers, contain *Sema6A* and *Sema6B* and repel *PlxnA4*-expressing mossy fibers to prevent their innervation into SR and SO. Whatever the subcellular localization of *Sema6A* and *Sema6B*, these two repellents play primary roles in proper projection of mossy fibers in CA3.

Many studies have addressed cellular and molecular mechanisms governing laminated afferent projections in the dentate molecular layer (for a review, see Förster et al., 2006). However, less attention has been paid to the mechanisms that prevent mossy fibers from growing into the molecular layer. This study has demonstrated that *Sema6A* and *Sema6B* are required to prevent abnormal innervation of mossy fibers into the molecular layer. Furthermore, this study has shown that *Sema6A* and *Sema6B* suppress ectopic spreading of *PlxnA4*-expressing mossy cell axons to detain them at their correct target lamina. These findings indicate that *PlxnA4*-mediated repulsive signals of *Sema6A* and *Sema6B* also play crucial roles in neuronal circuit assembly in the dentate gyrus.

This study has shown that, in addition to *Sema6A* and *Sema6B*, other *PlxnA4*-related repellent(s) exist in SLM of CA3 and the outer molecular layer of the den-

tate gyrus to control proper projection of mossy fibers and mossy cell axons. It has been reported that cells of the entorhinal cortex secrete a diffusible repellent for mossy fibers *in vitro* (Chédotal et al., 1998). Therefore, entorhinal fibers in SLM and the outer molecular layer might themselves contain common *PlxnA4*-related repellent(s) to suppress aberrant projection of mossy fibers and mossy cell axons.

Attraction of mossy fibers by *PlxnA2* and unknown factor(s) in CA3

Why can mossy fibers normally innervate into CA3, where potent mossy fiber repellents, *Sema6A* and *Sema6B*, are expressed? As discussed above, repulsive activities of *Sema6A* are attenuated by *PlxnA2* in proximal parts but not distal parts of the suprapyramidal region. Furthermore, this study has revealed that the *Sema6B* response on mossy fibers is not attenuated by *PlxnA2*. Therefore, attractive guidance mechanisms that compensate for

the semaphorin-induced mossy fiber repulsion and promote innervation of mossy fibers into CA3 would be required. This study has shown that *PlxnA2* itself promotes outgrowth of mossy fibers *in vitro* (Fig. 8A). The suprapyramidal bundle is slightly thicker in *Sema6A* mutants than in *PlxnA2;Sema6A* double mutants (Fig. 8B), suggesting that the growth-promoting activity of *PlxnA2* plays a practical role in the attraction of mossy fibers.

PlxnA2 propagates repulsive signals of class 3 semaphorins by forming receptor complexes with neuropilins (Takahashi et al., 1999). *PlxnA2* also serves as a direct receptor for *Sema6A* and/or *Sema6B* in embryonic spinal motor neurons (Bron et al., 2007), developing cerebellar granule cells (Renaud et al., 2008), and cardiac neural crest cells (Toyofuku et al., 2008) to regulate migration and positioning of these cells. In contrast, in developing hippocampus *PlxnA2* does not function as a receptor for repellents, but rather works as a neuronal attractant. It is an open question how *PlxnA2* promotes growth of mossy fibers. It has been shown that plexin-A1 (Ohta et al., 1995) and plexin-B3 (Hartwig et al., 2005) induce cell adhesion by homophilical interaction and, furthermore, that the homophilical interaction of plexin-B3 enhances neurite outgrowth of cerebellar neurons (Hartwig et al., 2005). Therefore, one possibility is that *PlxnA2* promotes outgrowth of mossy fibers via its *trans*-homophilical interaction. It has been shown that plexin-A1 functions as not only a receptor but also as a ligand for *Sema6D* in cardiac morphogenesis (Toyofuku et al., 2004). Therefore, the alternative is that growth-promoting activities of *PlxnA2* would be mediated via receptor(s) in mossy fibers. Identification of binding partners for *PlxnA2* is required to understand further functions of *PlxnA2* in mossy fiber projection.

In *PlxnA2;Sema6A* and *PlxnA2;Sema6B* double mutants, in which *PlxnA2* is deprived while *Sema6A* or *Sema6B* remain intact, many mossy fibers innervate into proximal parts of the suprapyramidal region (Fig. 8B). These results indicate that other mossy fiber attractant(s) exist in proximal parts of the suprapyramidal region. We refer to the attractant as pan-mossy fiber attractant, PMFA (Fig. 8A). It has been reported that netrin-1 is expressed in pyramidal cells and can attract mossy fibers *in vitro* (Steup et al., 2000). A more recent study has shown that functional blocking of netrin-1 by specific antibodies results in the attenuation of mossy fiber growth toward CA3 in slice cultures (Muramatsu et al., 2010). Therefore, netrin-1 is a most likely candidate for PMFA. Similarly to mossy fibers in *PlxnA2* mutant mice, mossy fibers in mice deficient for the neural cell adhesion molecule (NCAM) (Cremer et al., 1997) and the transcription factor serum response factor (SRF) (Knöll et al., 2006) do not

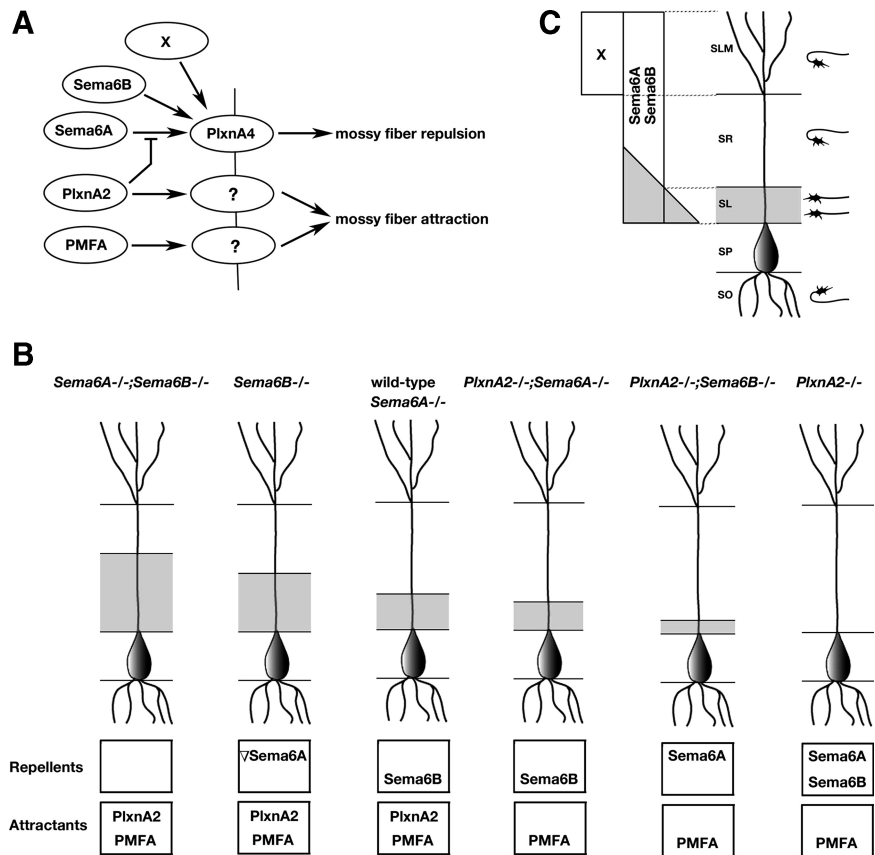


Figure 8. Summary of functions of repellents and attractants in laminar projection of mossy fibers. **A**, Repulsive and attractive signals that regulate mossy fibers projection. *PlxnA4* is expressed in mossy fibers and serves as a receptor for two neuronal repellents, *Sema6A* and *Sema6B*, which are expressed in CA3. *PlxnA4* also mediates mossy fiber repellent(s), *X*, which is expressed in SLM. *PlxnA2* in CA3 competitively suppresses the *Sema6A*-*PlxnA4* interaction and thereby attenuates *Sema6A*-induced mossy fiber repulsion. On the other hand, *PlxnA2* itself and unknown molecule(s) in CA3 (PMFA; see Discussion) function as attractants for mossy fibers. Receptors that mediate attractive signals of *PlxnA2* and PMFA have not been determined (see Discussion). **B**, Schematic diagrams of the mossy fiber projection patterns in the suprapyramidal region of CA3ab in wild-type mice, *Sema6A*, *Sema6B*, and *PlxnA2* mutant mice, and double knock-out mice for these genes. The area to which mossy fibers project is represented by the color gray. Mossy fiber repellents and attractants that have remained intact are given for each mouse line. Mossy fiber repellent, *X*, in SLM is omitted. Repulsive activities of *Sema6A* would remain intact in *PlxnA2*-deficient mouse lines: *PlxnA2*^{-/-}; *Sema6B*^{-/-} and *PlxnA2*^{-/-}. On the other hand, *Sema6A* activities would be completely attenuated by *PlxnA2* in wild-type mice and partially in *Sema6B*^{-/-} mice (see Discussion). The active *Sema6A* in *Sema6B*^{-/-} mice is represented as ∇ *Sema6A*. **C**, A model for the laminar projection of mossy fibers. The model shows that the relative strength of mossy fiber repulsion by *Sema6A* and *Sema6B* and attraction by *PlxnA2* and PMFA (represented in sum by gray color) determines the areas permissive for mossy fibers to innervate into the suprapyramidal region of CA3ab. Mossy fiber repellent, *X*, in SLM also suppresses innervation of mossy fibers into the lamina.

grow into the suprapyramidal and infrapyramidal regions but terminate within SP. Therefore, NCAM or SRF target genes might also function as PMFA.

Balance between repulsion and attraction of mossy fibers prescribes the areas permissive for mossy fibers to grow in CA3

On the basis of above discussion, we propose a model showing how mossy fiber repulsion by *Sema6A* and *Sema6B* and attraction by *PlxnA2* and PMFA prescribe the area permissive for mossy fibers to grow in the suprapyramidal region (Fig. 8C). In the model, we assume that mossy fiber repellents, *Sema6A* and *Sema6B*, are evenly distributed throughout the suprapyramidal region. We also assume that mossy fiber attractants, *PlxnA2* and PMFA, are distributed in a proximodistal gradient as a whole, although chemical nature of PMFA has been unknown. The model shows that the target lamina for mossy fibers in the supra-

pyramidal region is not based on absolute levels of single molecules but is determined by relative balance of mossy fiber repulsion and attraction; mossy fibers innervate the areas where attractive forces overwhelm repulsive forces. In *Sema6A*;*Sema6B* double mutants that lack repellents, mossy fibers spread throughout the area where mossy fiber attractants are distributing (Fig. 8B). In *PlxnA2* mutants, repulsive forces by Sema6A and Sema6B overwhelm attractive force by PMFA, and therefore mossy fibers are prevented from innervating the suprapyramidal region (Fig. 8B). Discrete target selection of motor axons in *Drosophila* is conducted by this general principle of axon guidance, with antagonistic guidance signals being produced from the same region (Winberg et al., 1998).

The above model does not explain why mossy fibers directly innervate into SR in *Sema6B*-deficient mouse lines (Figs. 2F, 7B) and why the fibers innervate into the infrapyramidal region of CA3c in all mutant mouse lines examined. Additional attractants for mossy fibers or factors that compensate the Sema6A- and Sema6B-induced mossy fiber repulsion might exist in CA3c.

References

- Amaral DG, Dent JA (1981) Development of the mossy fibers of the dentate gyrus. I. A light and electron microscopic study of the mossy fibers and their expansions. *J Comp Neurol* 191:51–86.
- Amaral DG, Witter MP (1995) Hippocampal formation. In: *The rat nervous system* (Paxinos G, ed), pp 443–493. New York: Academic.
- Bagri A, Cheng HJ, Yaron A, Pleasure SJ, Tessier-Lavigne M (2003) Stereotyped pruning of long hippocampal axon branches triggered by retraction inducers of the semaphorin family. *Cell* 113:285–299.
- Barallobre MJ, del Río JA, Alcántara S, Borrell V, Aguado F, Ruiz M, Carmona MA, Martín M, Fabre M, Yuste R, Tessier-Lavigne M, Soriano E (2000) Aberrant development of hippocampal circuits and altered neural activity in netrin 1-deficient mice. *Development* 127:4797–4810.
- Borrell V, Puiadas L, Simó S, Durà D, Solé M, Cooper JA, Del Río JA, Soriano E (2007) Reelin and mDab1 regulate the development of hippocampal connections. *Mol Cell Neurosci* 36:158–173.
- Brinks H, Conrad S, Vogt J, Oldekamp J, Sierra A, Deitinghoff L, Bechmann I, Alvarez-Bolado G, Heimrich B, Monnier PP, Mueller BK, Skutella T (2004) The repulsive guidance molecule RGMA is involved in the formation of afferent connections in the dentate gyrus. *J Neurosci* 24:3862–3869.
- Bron R, Vermeren M, Kokot N, Andrews W, Little GE, Mitchell KJ, Cohen J (2007) Boundary cap cells constrain spinal motor neuron somal migration at motor exit points by a semaphorin-plexin mechanism. *Neural Dev* 2:21–39.
- Chédotal A, Del Río JA, Ruiz M, He Z, Borrell V, de Castro F, Ezan F, Goodman CS, Tessier-Lavigne M, Sotelo C, Soriano E (1998) Semaphorins III and IV repel hippocampal axons via two distinct receptors. *Development* 125:4313–4323.
- Cheng HJ, Bagri A, Yaron A, Stein E, Pleasure SJ, Tessier-Lavigne M (2001) Plexin-A3 mediates semaphorin signaling and regulates the development of hippocampal axonal projections. *Neuron* 32:249–263.
- Cremer H, Chazal G, Goridis C, Represa A (1997) NCAM is essential for axonal growth and fasciculation in the hippocampus. *Mol Cell Neurosci* 8:323–335.
- Evan GI, Lewis GK, Ramsay G, Bishop JM (1985) Isolation of monoclonal antibodies specific for human c-myc proto-oncogene product. *Mol Cell Biol* 5:3610–3616.
- Förster E, Kaltschmidt C, Deng J, Cremer H, Deller T, Frotscher M (1998) Lamina-specific cell adhesion on living slices of hippocampus. *Development* 125:3399–3410.
- Förster E, Zhao S, Frotscher M (2006) Laminating the hippocampus. *Nat Rev Neurosci* 7:259–268.
- Goslin K, Asmussen H, Banker G (1998) Rat hippocampal neurons in low-density culture. In: *Culturing nerve cells* (Banker and G, Goslin K, eds), pp 339–370. Cambridge, MA: MIT.
- Hartwig C, Veske A, Krejčova S, Rosenberger G, Finckh U (2005) Plexin B3 promotes neurite outgrowth, interacts homophilically, and interact with Rin. *BMC Neurosci* 6:53–71.
- Kapfhammer JP, Raper JA (1987a) Collapse of growth cone structure on contact with specific neurites in culture. *J Neurosci* 7:201–212.
- Kapfhammer JP, Raper JA (1987b) Interactions between growth cones and neurites growing from different neural tissues in culture. *J Neurosci* 7:1595–1600.
- Katoh K, Takahashi Y, Hayashi S, Kondoh H (1987) Improved mammalian vectors for high expression of G418 resistance. *Cell Struct Funct* 12:575–580.
- Knöll B, Kretz O, Fiedler C, Alberti S, Schütz G, Frotscher M, Nordheim A (2006) Serum response factor controls neural circuit assembly in the hippocampus. *Nat Neurosci* 9:195–204.
- Leighton PA, Mitchell KJ, Goodrich LV, Lu X, Pinson K, Scherz P, Skarnes WC, Tessier-Lavigne M (2001) Defining brain wiring patterns and mechanisms through gene trapping in mice. *Nature* 410:174–179.
- Liu XB, Low LK, Jones EG, Cheng HJ (2005) Stereotyped axon pruning via plexin signaling is associated with synaptic complex elimination in the hippocampus. *J Neurosci* 25:9124–9134.
- Mitchell K, Pinson KI, Kelly OG, Brennan J, Zupicich J, Scherz P, Leighton PA, Goodrich LV, Lu X, Avery BJ, Tate P, Dill K, Pangilinan E, Wakenight P, Tessier-Lavigne M, Skarnes WC (2001) Functional analysis of secreted and transmembrane proteins critical to mouse development. *Nat Genet* 3:241–249.
- Mizuhashi S, Nishiyama N, Matsuki N, Ikegaya Y (2001) Cyclic nucleotide-mediated regulation of hippocampal mossy fiber development: a target-specific guidance. *J Neurosci* 21:6181–6194.
- Murakami Y, Suto F, Shimizu M, Shinoda T, Kameyama T, Fujisawa H (2001) Differential expression of plexin-A subfamily members in the mouse nervous system. *Dev Dyn* 220:246–258.
- Muramatsu R, Nakahare S, Ichikawa J, Watanabe K, Matsuki N, Koyama R (2010) The ration of ‘deleted in colorectal cancer’ to ‘uncoordinated-5A’ netrin-1 receptors on the growth cone regulates mossy fibre directionality. *Brain* 133:60–75.
- Nguyen-Ba-Charvet KT, Brose K, Marillat V, Kidd T, Goodman CS, Tessier-Lavigne M, Sotelo C, Chédotal A (1999) Slit2-mediated chemorepulsion and collapse of developing forebrain axons. *Neuron* 22:463–473.
- Ohta K, Mizutani A, Kawakami A, Murakami Y, Kasuya Y, Takagi S, Tanaka H, Fujisawa H (1995) Plexin: a novel neuronal cell surface molecule that mediate cell adhesion via a homophilic binding mechanism in the presence of calcium ions. *Neuron* 14:1189–1199.
- Otal R, Burgaya F, Frisen J, Soriano E, Martínez A (2006) Ephrin-A5 modulates the topographic mapping and connectivity of commissural axons in murine hippocampus. *Neurosci* 141:109–121.
- Pozas E, Pascual M, Nguyen-Ba-Charvet KT, Guijarro P, Sotelo C, Chédotal A, Del Río JA, Soriano E (2001) Age-dependent effects of secreted Semaphorins 3A, 3F, and 3E on developing hippocampal axons: in vitro effects and phenotype of Semaphorin 3A (–/–) mice. *Mol Cell Neurosci* 18:26–43.
- Renaud J, Kerjan G, Sumita I, Zagar Y, Georget V, Kim D, Fouquet C, Suda K, Sanbo M, Suto F, Ackerman SL, Mitchell KJ, Fujisawa H, Chédotal A (2008) Plexin-A2 and its ligand, Sema6A, control nucleus-centrosome coupling in migrating cerebellar granule cells. *Nat Neurosci* 11:440–449.
- Shimizu M, Murakami Y, Suto F, Fujisawa H (2000) Determination of cell adhesion sites of neuropilin-1. *J Cell Biol* 148:1283–1294.
- Skutella T, Nitsch R (2001) New molecules for hippocampal development. *Trends Neurosci* 24:107–113.
- Stein E, Savaskan NE, Ninnemann O, Nitsch R, Zhou R, Skutella T (1999) A role for the Eph ligand ephrin-A3 in entorhino-hippocampal axon targeting. *J Neurosci* 19:8885–8893.
- Steup A, Ninnemann O, Savaskan NE, Nitsch R, Püschel AW, Skutella T (1999) Semaphorin D acts as a repulsive factor for entorhinal and hippocampal neurons. *Eur J Neurosci* 11:729–734.
- Steup A, Lohrum M, Hamscho N, Savaskan NE, Ninnemann O, Nitsch R, Fujisawa H, Püschel AW, Skutella T (2000) Sema3C and netrin-1 differentially affect axon growth in the hippocampal formation. *Mol Cell Neurosci* 15:141–155.
- Suto F, Murakami Y, Nakamura F, Goshima Y, Fujisawa H (2003) Identification and characterization of a novel mouse plexin, plexin-A4. *Mech Dev* 120:385–396.
- Suto F, Ito K, Uemura M, Shimizu M, Shinkawa Y, Sanbo M, Shinoda T, Tsuboi M, Takashima S, Yagi T, Fujisawa H (2005) Plexin-A4 medi-

- ates axon-repulsive activities of both secreted and transmembrane semaphorins and plays roles in nerve fiber guidance. *J Neurosci* 25:3628–3637.
- Suto F, Tsuboi H, Kamiya H, Mizuno H, Kiyama Y, Komai S, Shimizu M, Sanbo M, Yagi T, Hiromi Y, Chédotal A, Mitchell KJ, Manabe T, Fujisawa H (2007) Interactions between plexin-A2, plexin-A4 and semaphorin 6A control lamina-restricted projection of hippocampal mossy fibers. *Neuron* 53:535–547.
- Takahashi T, Fournier A, Nakamura F, Wang LH, Murakami Y, Kalb RG, Fujisawa H, Strittmatter SM (1999) Plexin-Neuropilin-1 complexes form functional semaphorin-3A receptors. *Cell* 99:59–69.
- Toyofuku T, Zhang H, Kumanogoh A, Takegahara N, Suto F, Kamei J, Aoki K, Yabuki M, Hori M, Fujisawa H, Kikutani H (2004) Dual roles of Sema6D in cardiac morphogenesis through region-specific association of its receptor, Plexin-A1, with off-track and vascular endothelial growth factor receptor type 2. *Gen Dev* 18:435–447.
- Toyofuku T, Yoshida J, Sugimoto T, Yamamoto M, Makino N, Takamatsu H, Takegahara N, Suto F, Hori M, Fujisawa H, Kumanogoh A, Kikutani H (2008) Repulsive and attractive semaphorins cooperate to direct the navigation of cardiac neural crest cells. *Dev Biol* 321:251–262.
- Winberg ML, Mitchell KJ, Goodman CS (1998) Genetic analysis of the mechanisms controlling target selection: complementary and combinatorial functions of netrins, semaphorins, and IgCAMs. *Cell* 93:581–591.